Hybrid MacCormack and Implicit Beam-Warming Algorithms for a Supersonic Compression Corner

C. Ong* and D. Knight†
Rutgers, The State University of New Jersey, New Brunswick, New Jersey

A comparative study is made between the MacCormack explicit-implicit predictor-corrector and the Beam-Warming fully implicit algorithms for solving compressible viscous flow. The mass-averaged, two-dimensional compressible Navier-Stokes equations in strong conversation law form and general curvilinear coordinates are solved numerically by marching forth in time on a body-fitted curvilinear grid for a shock-wave/turbulent boundary-layer interaction over a two-dimensional compression corner. Computations are performed for a Mach number of 1.96 with a Reynolds number Re_{δ_∞} (based on the incoming boundary-layer thickness δ_∞) of 0.25×10^6 and for a Mach number of 2.83 with a Reynolds number of 1.8×10^6. The primary objectives of the study are 1) to determine the extent to which the steady-state solution obtained by the hybrid MacCormack algorithm is dependent upon the size of the time step employed in marching the calculation toward the steady-state solution, 2) to compare the two algorithms regarding accuracy and efficiency, and 3) to further examine the efficacy of the Baldwin-Lomax algebraic turbulent eddy-viscosity model through comparison with recent experimental measurements of the Reynolds shear stress.

Introduction

UNTIL the mid-1970's, most numerical schemes used to solve the Navier-Stokes equations were explicit algorithms such as MacCormack's explicit method.[1] The restriction placed on the size of the maximum allowable time step severely limited the usefulness of explicit procedures in the solution of high Reynolds number compressible flow. By the mid-1970's this [Courant-Friedrichs-Lewy (CFL)] restriction was removed by the fully implicit numerical schemes of Briley and McDonald[2] and Beam and Warming[3] which became very widely used. However, these implicit methods require linearization of terms in the governing equations in order to form desirable block matrix structures. The resulting block pentadiagonal or septadiagonal matrices need to be approximately factored into block tridiagonal matrices before an efficient matrix inversion procedure can be applied. Both of these approximations result in limitations to the size of the maximum allowable time step.[4]

In 1981 MacCormack[5] presented an explicit-implicit predictor-corrector method that involved the simple inversion of block bidiagonal matrices in an effort to reduce computer time. Since its introduction, the hybrid scheme has been used by numerous investigators to compute a large variety of compressible viscous flows. In calculating a separated shock-wave/laminar boundary-layer interaction over a flat plate, MacCormack was able to reduce the required computer time by a factor of 17.5 relative to his fully explicit method while maintaining comparable accuracy. Shang and MacCormack[6] evaluated the new method against its fully explicit predecessor for a Mach 8 flow over an axisymmetric biconic body and achieved computer time reduction by a factor of 13.

Accuracy and efficiency are but two features desirable in a numerical method; independence of the steady-state solution from the size of the chosen time step is another. Before asking whether the steady-state solution of a given numerical algorithm is accurate, it seems logical to first inquire if it yields the same steady-state solution, regardless of the time-step size selected. MacCormack advocated[5,7] a succesive reduction of the time-step size near the end of the calculation of high Reynolds number flows in order to avoid any possible dependence of the steady-state solution on the time-step size. This concern about time-step dependence was underscored by Kumar,[8] who reported finding considerable time-step dependence of his steady-state solution near the immediate neighborhood of a separation region induced by shock impingement upon the turbulent boundary layer in a duct whose inflow Mach numer was 5. However, no significant CFL dependence was found by Gupta et al.,[9] who computed an unseparated laminar flow over an axisymmetric body, in the presence of a detached bow shock, at a Mach number of 44.

Other investigators who used MacCormack's explicit-implicit scheme included Kordulla and MacCormack,[10] White and Anderson,[11] Hung and Kordulla,[12] and Imlay et al.[13] Despite the indication of possible significant CFL dependence of the steady-state solution by MacCormack and Kumar, few investigators have addressed this issue, and some have stated without further substantiation that "the implicit MacCormack method is unreliable such that the steady-state solutions depend on time increments."[14] Nevertheless, it is obviously important to ascertain the severity of any such dependence. Hence, the first objective of the present study is to determine whether the steady-state solution obtained by the MacCormack explicit-implicit method depends on the time-step size.

Since the Beam-Warming method has become very popular and the explicit-implicit hybrid method appears to be accurate and efficient, the question regarding their relative accuracy and efficiency is clearly a relevant and important one. Lawrence et al.[15] discussed this issue in the case of the Mach 2 laminar flow over a flat plate. They used both algorithms to solve the parabolized Navier-Stokes equations by space marching. They observed that the computer time requirements for the Beam-Warming and MacCormack hybrid were approximately equal. However, a more extensive study for a time-marching solution of the full two-dimensional Navier-Stokes equations over a realistic grid appears necessary. Thus, the second objective of

Received Nov. 22, 1985; presented as Paper 86-0204 at the AIAA 24th Aerospace Sciences Meeting, Reno, NV, Jan. 6–9, 1986; revision received June 27, 1986.

*Graduate Student, Department of Mechanical and Aerospace Engineering; presently at Continuum Dynamics, Inc., Princeton, NJ. Member AIAA.

†Professor, Department of Mechanical and Aerospace Engineering. Associate Fellow AIAA.

the present study is an accuracy and efficiency comparison between the MacCormack explicit-implicit and the Beam-Warming fully implicit algorithms.

The configuration selected for this comparative study is supersonic turbulent flow past a two-dimensional compression corner (Fig. 1). Extensive experimental measurements have been performed by Settles et al.[16] for the specific case of a Mach 2.83 turbulent flow past a two-dimensional compression corner at a series of corner angles $\alpha = 8$ to 24 deg, and for a range of Reynolds numbers $Re_{\delta_\infty} = 0.76 \times 10^6$ to 7.7×10^6. The measurements of Settles et al.[16] include surface pressure, skin friction, surface oil flow visualization, and boundary-layer profiles of velocity, static pressure, and Mach number. Visbal[17] and Visbal and Knight[18] computed the entire set of flows corresponding to the experimental configurations of Settles et al. utilizing the algebraic turbulent eddy-viscosity of Baldwin and Lomax. It was observed that 1) the Baldwin-Lomax outer function was unsuitable for determination of the length scale of the turbulence in the separation region; 2) incorporation of the relaxation model of Shang and Hankey[19] improved the prediction of the extent of upstream propagation of the disturbance associated with the corner; and 3) the computed boundary-layer recovery, downstream of reattachment, was significantly less than that observed experimentally.

Recently, measurements of turbulent Reynolds stresses have been performed for the same configuration.[20-22] These measurements, therefore, provide the opportunity for direct examination of the efficacy of the Baldwin-Lomax turbulence model. Hence, the third objective of the present study is to compare directly the computed and measured Reynolds shear stress for the two-dimensional compression corner at Mach 2.83 for several corner angles and to attempt to elucidate the deficiencies in the Baldwin-Lomax model. In addition, computations have been performed for the two-dimensional compression corner at Mach 1.96 and $Re_{\delta_\infty} = 0.25 \times 10^6$ for $\alpha = 16$ deg, and the results have been compared with the experimental data of Dolling[23] for surface pressure.

Method of Solution

Governing Equations

The flow was assumed to be described by the two-dimensional, mass-averaged compressible Navier-Stokes equations. The equations were written in strong conservation law form and general curvilinear coordinates.[24,25] The fluid was assumed to be a perfect gas with a molecular dynamic viscosity given by Sutherland's law and a constant molecular Prandtl number of 0.72.

Turbulence was simulated by the Baldwin-Lomax[26] algebraic eddy-viscosity model with $\kappa = 0.40$, $A^+ = 26$, $C_{\text{Kleb}} = 0.3$, and $k = 0.0168$. The value of C_{cp} was obtained from the investigation of York and Knight[27] and Visbal,[17] which detailed the dependence of C_{cp} on Mach number. In particular, C_{cp} varies from 1.8 at Mach 2 to 2.1 at Mach 3. The relaxation model of Shang and Hankey[19] was employed in all cases except the 8-deg compression ramp at Mach 2.83, with the relaxation length scale set equal to the upstream boundary-layer thickness. The turbulent Prandtl number is 0.9.

Computational Domain and Boundary Conditions

Nearly orthogonal, body-fitted grids were generated using the method of Visbal and Knight.[28] Typically, 30 grid points were contained within the incoming boundary layer, and the distance between the wall and the nearest line of grid points had a Y^+ value smaller than 2.5, where Y^+ is the distance normal to the wall nondimensionalized by the local friction velocity and the wall value of the kinematic viscosity. For each flow configuration, the same grid was employed for the calculations using the Beam-Warming and the MacCormack hybrid algorithms.

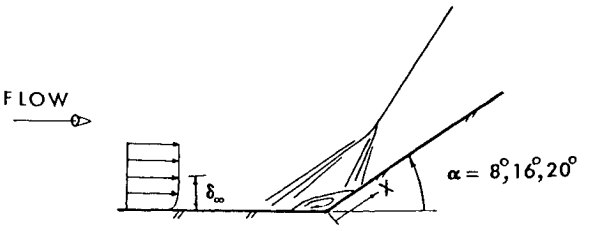

Fig. 1 Flow geometry.

The inflow boundary was positioned in the undisturbed, turbulent flat-plate boundary layer where the computed momentum thickness matched the experimental value. In both the Beam-Warming and the hybrid MacCormack computations, the flow variables on the inflow boundary were held fixed at the given values. The inflow boundary condition for the implicit step of the hybrid MacCormack was prescribed by setting the temporal change in the solution[5] $\delta \boldsymbol{U}$ to zero. The outflow boundary was located far enough downstream of the corner to be in a region of small streamwise flow gradients. Along the outflow boundary, the extrapolation condition was assumed. For this boundary, both the Beam-Warming and the explicit step of the hybrid MacCormack represented $\partial \boldsymbol{U}/\partial \xi = 0$ by a first-order accurate differencing, where ξ is the transformed coordinate in the general streamwise direction and $\boldsymbol{U}$ is the vector of dependent variables.[3,5] The implicit part of MacCormack's method set the temporal change $\delta \boldsymbol{U}$ at the downstream boundary equal to its value at the adjacent constant-ξ line. At the lower boundary, the velocity and normal derivative of the static pressure were set to zero. For the Mach 1.96 compression corner flow, adiabatic boundary conditions were used for both schemes, whereas a constant (near adiabatic) temperature was specified for the Mach 2.83 corner. The lower boundary condition for the implicit portion of MacCormack's hybrid was formulated by allowing a one-half time-step lag in the value of the temporal change $\delta \boldsymbol{U}$. The upper boundary was placed sufficiently far from the lower so that freestream conditions prevailed all along its length. For the Beam-Warming scheme, a nonreflection condition[17] was applied. For the hybrid MacCormack, however, the flow variables along the upper boundary were simply held at the freestream value and $\delta \boldsymbol{U}$ was set to zero. The shock emerged through the outflow boundary.

Numerical Procedure

The fully implicit scheme studied was the approximate factorization algorithm of Beam-Warming,[3] formulated using Euler implicit time differencing and second-order-accurate centered differencing for the spatial derivatives. Fourth-order explicit damping terms were included in the manner shown by Thomas.[29] The explicit-implicit algorithm was that of MacCormack,[5] extended to two-dimensional general coordinates by von Lavante and Thompkins.[24] The algorithm is second-order-accurate in space and time. While marching in time, the order of finite differencing in the explicit predictor and corrector steps was cycled from one step to the next, whereas that in the implicit steps was kept as forward differencing in the predictor and backward in the corrector. At all times, opposite orders of differencing were employed in the predictor and corrector. The usual fourth-order damping, expressed in terms of the pressure, is used for the explicit part. Implicit damping was also incorporated, in the manner suggested by MacCormack.[5] Both the explicit-implicit[30] and fully implicit[17] computer codes were validated carefully with excellent accuracy for a variety of flows, including laminar and turbulent boundary layers and shock-wave/laminar boundary-layer interaction.

Results and Discussion

Courant Number Dependence of the Hybrid MacCormack

As indicated previously, the first objective of the research is to examine the possible Courant number dependence of the steady-state solution computed by the hybrid MacCormack algorithm. During this examination, it will be convenient to examine also the accuracy of the solution in comparison with the Beam-Warming results and the experimental measurements of Dolling[23] and Settles et al.[16]

Mach 1.96 Flow Over 16-Deg Compression Corner

The computed and measured surface pressure distributions for the Mach 1.96 compression corner are displayed in Fig. 2. The Reynolds number $Re_{\delta_\infty} = 0.25 \times 10^6$ and $\alpha = 16$ deg. In this and all subsequent figures, X denotes the distance from the corner measured along the surface. Calculated profiles are for the MacCormack hybrid method at Courant numbers of 0.9 (fully explicit) and 45 (hybrid), and the Beam-Warming algorithm, where the Courant number is defined by Shang.[31] The experimental data of Dolling[23] are also depicted. The results clearly indicate that the steady-state solution for the surface pressure using the MacCormack explicit-implicit algorithm is insensitive to the Courant number and very close to the Beam-Warming results. The computed upstream propagation of the surface pressure, measured from the corner ($X = 0$), is approximately 30% below the experimental value. Since the extent of the computed upstream propagation is related directly to the magnitude of the length scale employed in the relaxation model, the employed length scale of δ_∞ is too small for this case. The present results at Mach 2 for $Re_{\delta_\infty} = 0.25 \times 10^6$, together with previous results of Visbal and Knight[18] at Mach 3 for $Re_{\delta_\infty} = 0.76 \times 10^6$ to 7.7×10^6, imply that the relaxation length is a moderate function of Re_{δ_∞} (i.e., the relaxation length[17] increases with decreasing Re_{δ_∞}). This observation is consistent with the results of Shang and Hankey,[19] who employed a relaxation length of $10\delta_\infty$ for their studies of the two-dimensional compression corner at Mach 3 for $Re_{\delta_\infty} = 0.14 \times 10^6$.

The calculated skin-friction coefficient c_f distribution for the same flow is shown in Fig. 3. The computed results, using the MacCormack hybrid algorithm, are observed again to have no marked dependence on the Courant number, despite the fact that the two Courant numbers differ by a factor of 50. The computed results are in good agreement with the computation using Beam-Warming's fully implicit algorithm. The results using McCormack's method manifest a small streamwise oscillation in c_f downstream of reattachment. The cause of this oscillation requires further investigation.

Mach 2.83 Flow Over 16-Deg Compression Corner

The surface pressure distribution for a Mach 2.83 flow at $Re_{\delta_\infty} = 1.6 \times 10^6$ and $\alpha = 16$ deg are shown in Fig. 4 for computations using the methods of MacCormack and Beam-Warming. The experimental measurements of Settles et al.[16] are also displayed. A high Courant number of 85 and a low of 30 used by the hybrid algorithm give no discernible difference in the computed surface pressure. There is also good agreement with the pressure calculated using the Beam-Warming scheme, as well as with experiment.

In Fig. 5, the corresponding skin-friction distributions are exhibited. As before, the skin friction computed by the hybrid method is insensitive to the time-step size. There is a slight tendency for the higher CFL case to predict a marginally lower skin friction further downstream from reattachment. The hybrid method predicts a skin friction modestly higher than the Beam-Warming method further downstream from reattachment, but agrees closely with the latter practically everywhere else.

Mach 2.83 Flow Over 20-Deg Compression Corner

The surface pressure for the Mach 2.83 flow at $Re_{\delta_\infty} = 1.6 \times 10^6$ and $\alpha = 20$ deg is detailed in Fig. 6. This ramp angle is the largest studied in this investigation. The Courant numbers used for the MacCormack scheme are 30 and 70. The Beam-Warming and experimental results[16] are also plotted. As in the previous cases, the computed surface pressure exhibits no Courant number dependence for the MacCormack algorithm. In addition, the results obtained from the Beam-Warming and MacCormack hybrid algorithms are in close agreement.

In Fig. 7 the skin friction for the same flow is shown for the MacCormack and Beam-Warming methods as well as the experiment. The results indicate that, even in the presence of such a strong adverse pressure gradient and large separation region, the computed skin friction is insensitive to time-step size. The hybrid method predicts a skin friction slightly higher than the Beam-Warming scheme downstream of reattachment.

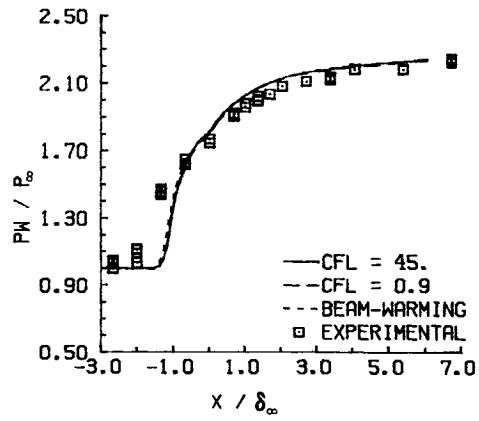

Fig. 2 Surface pressure for Mach 1.96 flow over 16-deg ramp.

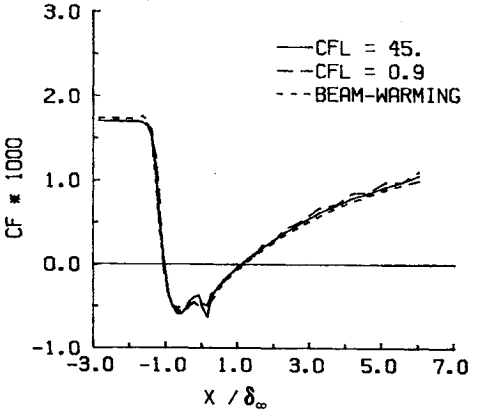

Fig. 3 Skin friction for Mach 1.96 flow over 16-deg ramp.

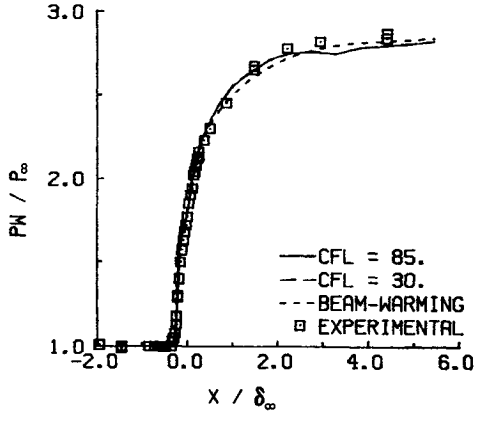

Fig. 4 Surface pressure for Mach 2.83 flow over 16-deg ramp.

Efficiency of the Hybrid MacCormack Algorithm

In addition to Courant number dependence and accuracy, the efficiency of the hybrid McCormack algorithm was examined also for the Mach 1.96 flow over a 16-deg ramp. Computations using the hybrid scheme were made at Courant numbers of 0.9 (fully explicit), 5, 10, 21, 40, and 45. One computation using the Beam-Warming scheme was performed employing a maximum Courant number of 33. In order to avoid numerical instability, it was necessary to start the Beam-Warming calculation at a smaller time step and progressively increase it to a maximum consistent with numerical stability. Both numerical codes were written in FORTRAN and executed on an NAS AS/9000 mainframe computer. A uniform set of convergence criteria was employed for all calculations. It was observed that convergence to steady state required approximately the same physical time of integration in all cases.

The computer time requirements for these computations are tabulated in Table 1. It is observed for this case that the hybrid scheme requires one-third of the computer time used by the Beam-Warming method, and up to a factor of 36 less than the fully explicit MacCormack algorithm.

Reynolds Shear-Stress Comparison

In the present section, the computed and experimental profiles for the Reynolds shear stress, defined as $-\bar{\rho}\overline{u'v'}$, are displayed. The quantities u' and v' are the temporal fluctuating velocity components parallel and normal to the wall, respectively. The overbar represents the time average. The experimental Reynolds shear stress is obtained from the measurements[20,22] of $-\overline{(\rho u)'v'}$ by employing the "Strong Reynolds Analogy" (i.e., pressure fluctuations are small compared to density or temperature fluctuations) and the "Very Strong Reynolds Analogy" (i.e., fluctuations in total temperature are neglected). The uncertainties (approximately $\pm 30\%$) in the measurement of the Reynolds stress are discussed in Refs. 20-22. The theoretical Reynolds shear stress, modeled using the Baldwin-Lomax algebraic turbulent eddy viscosity, is $-\overline{\rho u''v''}$, where u'' and v'' denote the mass-averaged fluctuating velocity components parallel and normal to the wall, respectively. With the assumption of the Strong and Very Strong Reynolds analogies, the theoretical Reynolds shear stress is equal approximately to $-\bar{\rho}\overline{u'v'}$. In all plots, the experimental and theoretical Reynolds shear stress are normalized by $0.5\ \rho_\infty U_\infty^2$.

Mach 2.83 Flow Over 16-Deg Compression Corner

For the Mach 2.83 flow over a 16-deg compression corner, the calculated and experimental Reynolds stress profiles at stations $X/\delta_\infty = 0.49$ and 5.4 are exhibited in Figs. 8 and 9. It is apparent that the peaks of the computed and experimental Reynolds stress profiles are comparable in magnitude. This is summarized in Fig. 10, which displays the distribution of the

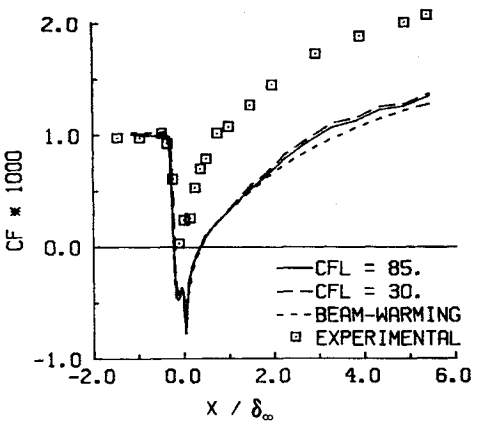

Fig. 5 Skin friction for Mach 2.83 flow over 16-deg ramp.

Table 1 Computer time comparison, Mach 1.96 flow over 16-deg ramp

Algorithm	CFL no.[31]	Computer time, h (NAS AS/9000)
Beam-Warming	33.0	8.7
MacCormack	45.0	2.9
explicit-implicit	40.0	3.2
hybrid	21.0	6.0
	10.0	11.8
	5.0	12.4
	0.9 (Explicit)	104.1

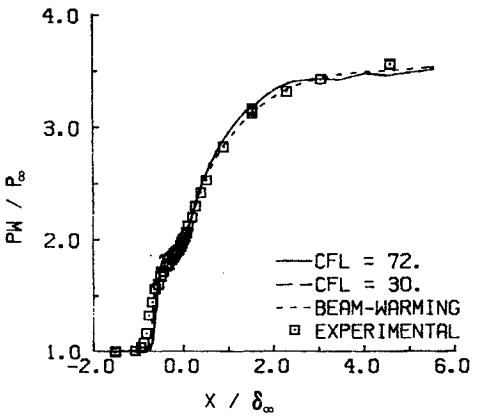

Fig. 6 Surface pressure for Mach 2.83 flow over 20-deg ramp.

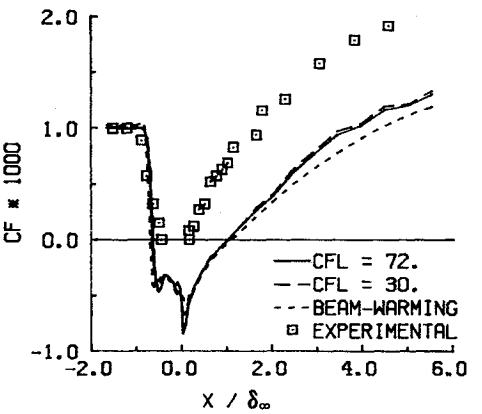

Fig. 7 Skin friction for Mach 2.83 flow over 20-deg ramp.

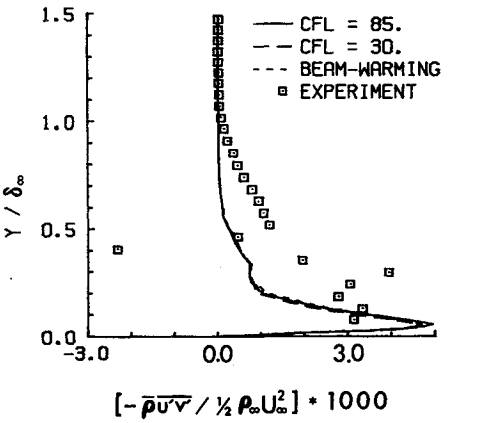

Fig. 8 Reynolds shear stress at $X/\delta_\infty = 0.49$ for Mach 2.83 over 16-deg ramp.

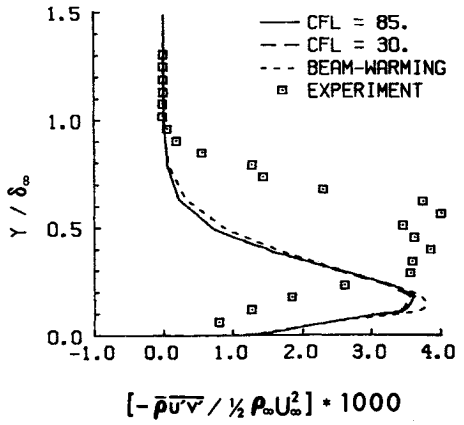

Fig. 9 Reynolds shear stress at $X/\delta_\infty = 5.4$ for Mach 2.83 flow over 16-deg ramp.

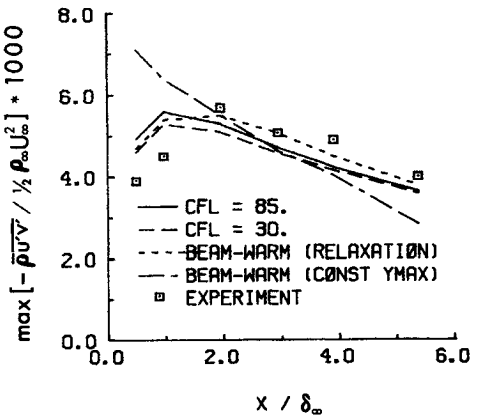

Fig. 10 Magnitude of peak of the Reynolds stress for Mach 2.83 over 16-deg ramp.

magnitude of the peak of the Reynolds stress profiles with distance X. It is evident, however, that the computed peak is located too close to the wall. The height of the peak Y_{peak} as a function of distance X is displayed in Fig. 11. The distance of the peak from the wall increases as the boundary layer develops downstream for both computed and experimental profiles.

Mach 2.83 Flow Over 20-Deg Compression Corner

In Figs. 12 and 13, the profiles of the Reynolds shear stress at stations $X/\delta_\infty = 1.0$ and 4.6 are shown for the Mach 2.83 flow over a 20-deg compression corner. The distribution of the peak of the Reynolds stress profile is exhibited in Fig. 14. It shows that, although the experimental peak remains approximately constant, the computed peak steadily diminishes. In Fig. 15, the corresponding distribution of the location of the peak Y_{peak} of the Reynolds stress profile is displayed. A pronounced underprediction of the distance of the peak from the wall is evident, similar to that observed in Fig. 11 for the 16-deg corner.

Discussion of Comparison of Reynolds Stress Profiles

In summarizing the preceding comparison of Reynolds shear stress, the principal discrepancy is the underprediction of the height of its peak. The Baldwin-Lomax model is modestly successful in predicting the magnitude of the peak of the Reynolds shear stress, although the success is tempered for $\alpha = 20$ deg by an apparent incorrect trend in X.

Recognizing the inherent simplicity and limitations of the mixing length concept, it is interesting, nonetheless, to attempt to treat the defects of the Baldwin-Lomax model "symptomatically." It is noted in Fig. 15 that the height of the peak

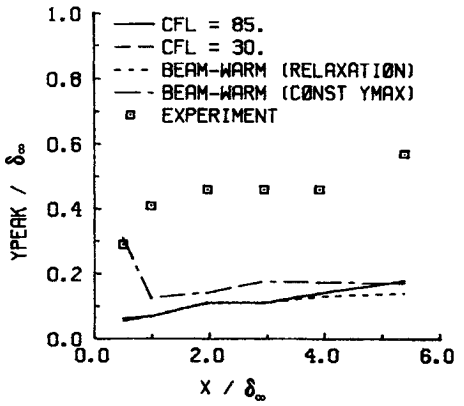

Fig. 11 Location of peak in Reynolds shear-stress profile for Mach 2.83 flow over 16-deg ramp.

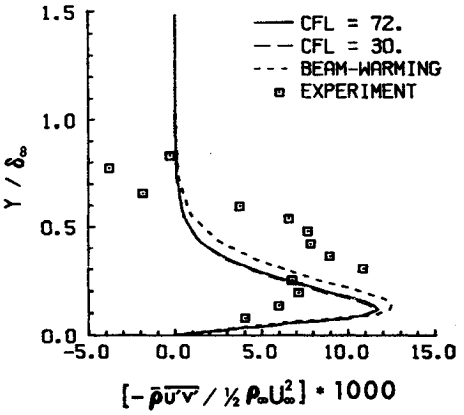

Fig. 12 Reynolds shear stress at $X/\delta_\infty = 1.0$ for Mach 2.83 flow over 20-deg ramp.

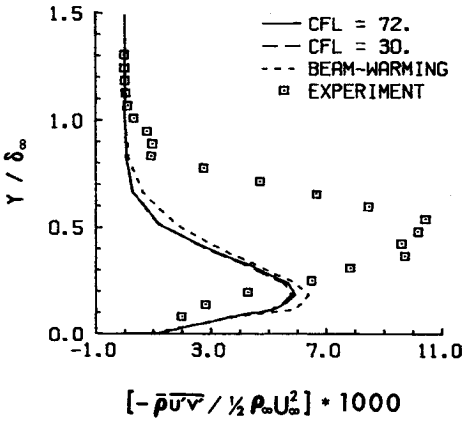

Fig. 13 Reynolds shear stress art $X/\delta_\infty = 4.6$ for Mach 2.83 flow over 20-deg ramp.

Y_{peak} of the computed Reynolds shear stress correlates with the magnitude of the computed outer length scale Y_{max} of the Baldwin-Lomax model for $\alpha = 20$ deg; a similar observation applies for $\alpha = 16$ deg. The location of the experimental peak Reynolds stress corresponds to the outer portion of the boundary layer (i.e., outside the point where the Baldwin-Lomax model switches from the inner to the outer formulation). This suggests, therefore, that the computed Reynolds shear stress may be improved by increasing Y_{max}. This approach was attempted by Visbal and Knight[18] for $\alpha = 16$ deg. Specifically, Y_{max} was kept constant at its upstream value; this

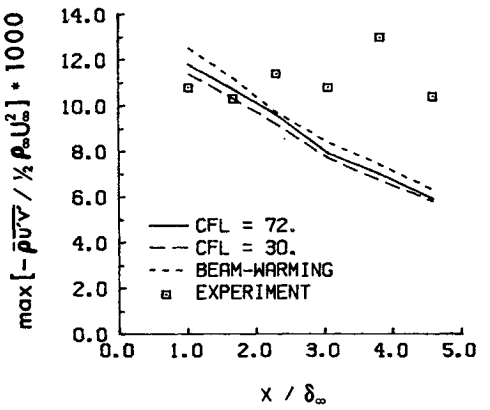

Fig. 14 Magnitude of peak of the Reynolds stress for Mach 2.83 flow over 20-deg ramp.

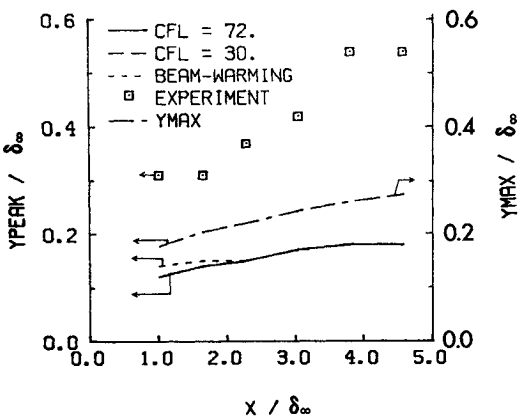

Fig. 15 Baldwin-Lomax length scale Y_{max} and location of the peak of the Reynolds shear stress for Mach 2.83 flow over 20-deg ramp.

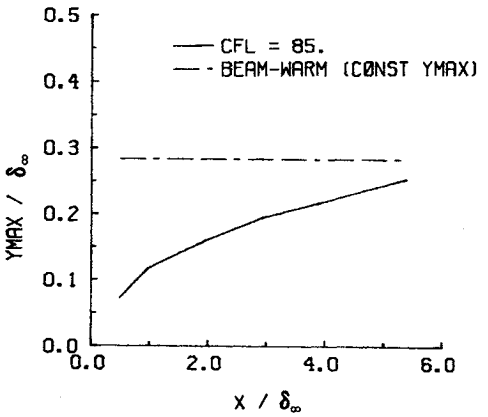

Fig. 16 Baldwin-Lomax length scale Y_{max} for Mach 2.83 flow over 16-deg ramp.

represents an increase in Y_{max} compared to the calculations with the relaxation eddy-viscosity model (Fig. 16). The effect of increasing Y_{max} is seen in Figs. 10 and 11. The magnitude of the peak Reynolds shear stress is overpredicted for $X < 2\delta_\infty$, whereas a slight improvement in Y_{peak} is noted. The computed Reynolds shear stress profiles[30] display a double-peaked behavior at $X/\delta_\infty = 0.49$ and 0.98, in disagreement with experiment. It may be concluded, therefore, that no *overall* improvement was obtained by increasing Y_{max}.

It is evident that the simple mixing-length Baldwin-Lomax model is incapable of accurately predicting the reattachment and downstream recovery of a separated two-dimensional compression corner flow. The model is based upon the concept of an equilibrium turbulent boundary layer exhibiting one characteristic velocity scale.[32] Downstream of reattachment, there are two characteristic velocity scales of the turbulence, namely, 1) an outer velocity scale associated with the turbulence fluctuations in the outer portion of the reattaching free shear layer; and 2) an inner velocity scale $u_* = [\tau_w(X)/\rho_w(X)]^{1/2}$ associated with the imposition of the no-slip boundary condition downstream of reattachment, which creates an "inside layer" within the boundary layer. The failure of the "simple" extension to the Baldwin-Lomax model previously described is not surprising within this framework. A more physically realistic turbulence model is required for two-dimensional separated compression corner flows which incorporates 1) the effect of the upstream history on the turbulent flow, and 2) the oscillatory motion of the shock-wave structure.[33,34] Regarding the first characteristic, the assumption of an algebraic eddy-viscosity model precludes the incorporation of the turbulence history, except through the crude technique of the relaxation model. Regarding the second characteristic, the Reynolds-averaged Navier-Stokes equations are formally capable of exhibiting large unsteadiness on a time scale T that is large compared to the energy-containing turbulent eddies (i.e., $T \gg \delta_\infty/U_\infty$). The measurements of Dolling et al.[33] exhibited features of the shock motion with time scales as large as $10\delta_\infty/U_\infty$. In each of the present calculations, the flowfield was integrated in time from an assumed initial condition using a time step less than $0.02\delta_\infty/U_\infty$. The time step, therefore, was sufficiently small to resolve any unsteadiness formally associated with the Reynolds-averaged equations. All calculations reached a steady-state solution with no evidence of shock-wave unsteadiness. Thus, the fact that neither the Beam-Warming nor the MacCormack scheme found an oscillating solution may be associated with a defect in the turbulence model, the numerical damping inherent in the algorithms, or the specific choice of initial conditions.

Conclusions

A comparative study has been performed for the MacCormack hybrid and the Beam-Warming fully implicit algorithms for a shock-wave/turbulent boundary-layer interaction over a two-dimensional corner. The computations employed identical grids and the Baldwin-Lomax algebraic turbulent eddy-viscosity model. It is observed that the steady-state solution of the MacCormack hybrid algorithm is remarkably insensitive to Courant number. The accuracy of the steady-state solution using MacCormack's hybrid algorithm is comparable to that of the Beam-Warming method for all cases. Based on experience with the Mach 1.96 computations, the MacCormack hybrid method is observed to reduce the computing time by a factor of up to 3 relative to the Beam-Warming method.

The computed Reynolds stress profiles are compared with the experimental data of Muck et al.[20-22] It is noted that the magnitude of the peak of the computed Reynolds shear stress is in approximate agreement with the measurements, although an apparent incorrect trend is evident for $\alpha = 20$ deg. The major discrepancy is the underprediction of the location of the peak of the computed Reynolds shear stress. It is found that a simple modification of the Baldwin-Lomax turbulence model involving an increase in the length scale Y_{max} of the outer eddy viscosity fails to demonstrate overall improvement. The Baldwin-Lomax model is based on the mixing-length concept and is incapable of accurately predicting the recovery of a separated two-dimensional compression corner flow. It is noted that several additional physical factors, omitted from the theoretical model, also affect the recovery of the boundary layer, including the history effect of the turbulence structure and the large-amplitude oscillatory motion of the shock structure.

Acknowledgments

This research is supported by the Air Force Office of Scientific Research under Grant AFOSR 82-0040, monitored by Dr. James Wilson.

References

[1] MacCormack, R.W., "The Effect of Viscosity in Hypervelocity Impact Cratering," AIAA Paper 69-354, 1969.

[2] Briley, W.R. and McDonald, H., "An Implicit Numerical Method for the Multi-dimensional Compressible Navier-Stokes Equations," United Aircraft Research Lab., East Hartford, CT, Rep. M911363-6, 1973.

[3] Beam, R. and Warming, R., "An Implicit Factored Scheme for the Compressible Navier-Stokes Equations," *AIAA Journal*, Vol. 16, April 1978, pp. 393–402.

[4] MacCormack, R.W., "Current Status of Numerical Solutions of the Navier-Stokes Equations," AIAA Paper 85-0032, 1985.

[5] MacCormack, R.W., "A Numerical Method for Solving the Equations of Compressible Viscous Flows," AIAA Paper 81-0110, 1981.

[6] Shang, J.S. and MacCormack, R.W., "Flow Over a Biconic Configuration with an Afterbody Compression Flap—A Comparative Numerical Study," AIAA Paper 83-1668, 1983.

[7] MacCormack, R.W., "Numerical Solution of the Equations of Compressible Viscous Flows," *Transonic, Shock, and Multidimensional Flows: Advances in Scientific Computing*, Academic Press, New York, 1982.

[8] Kumar, A., "Some Observations on a New Numerical Method for Solving the Navier-Stokes Equations," NASA TP-1934, 1981.

[9] Gupta, R.N., Gnoffo, P.A., and MacCormack, R.W., "A Viscous Shock-Layer Flowfield Analysis by an Explicit-Implicit Method," AIAA Paper 83-1423, 1983.

[10] Kordulla, W. and MacCormack R.W., "Transonic Flow Computations Using an Explicit-Implicit Method," *Proceedings of the 8th International Conference on Numerical Methods*, Aachen, Germany, 1982, pp. 286–295.

[11] White, M.E. and Anderson, J.D., "Application of MacCormack's Implicit Method to Quasi-One-Dimensional Nozzle Flows," AIAA Paper 82-0992, 1982.

[12] Hung, C.M. and Kordulla, W., "A Time-Split Finite-Volume Algorithm for 3-D Flow-Field Simulation," AIAA Paper 83-1957, 1983.

[13] Imlay, S.T., Kao, T.J., McMaster, D.L., and MacCormack, R.W., "Solution of the Navier-Stokes Equations for Flow Within a 2-D Thrust Reversing Nozzle," AIAA Paper 84-0344, 1984.

[14] Obayashi, S. and Kuwahara, K., "LU Factorization of an Implicit Scheme for the Compressible Navier-Stokes Equations," AIAA Paper 84-1670, 1984.

[15] Lawrence, S.L., Tannehill, J.C., and Chausee, D.S., "Application of the Implicit MacCormack Scheme to the Parabolized Navier-Stokes Equations," *AIAA Journal*, Vol. 22, Dec. 1984, pp. 1755–1763.

[16] Settles, G., Gilbert, R., and Bogdonoff, S., "Data Compilation for Shock Wave/Turbulent Boundary Layer Interaction Experiments on 2-D Compression Corners," Dept. of Aerospace & Mechanical Engineering, Princeton Univ., Princeton, NJ, Rep. MAE-1489, 1980.

[17] Visbal, M., "Numerical Simulation of Shock/Turbulent Boundary Layer Interactions over 2-D Compression Corners," Ph.D. Thesis, Dept. of Mechanical and Aerospace Engineering, Rutgers Univ., New Brunswick, NJ, 1983.

[18] Visbal, M. and Knight, D., "The Baldwin-Lomax Turbulence Model for 2-D Shock-Wave/Boundary-Layer Interactions," *AIAA Journal*, Vol. 22, July 1984, pp. 921–928.

[19] Shang, J.S. and Hankey, W.L., "Numerical Solutions for Supersonic Turbulent Flow Over a Compression Ramp," *AIAA Journal*, Vol. 13, Oct. 1975, pp. 1360–1374.

[20] Muck, K.C., Hayakawa, K., and Smits, A.J., "Compilation of Turbulence Data for a 20° Compression Corner at Mach 2.9," Dept. of Mechanical and Aerospace Engineering, Princeton Univ., Princeton, NJ, MAE Rep. 1620, 1983.

[21] Muck, K.C., Hayakawa, K., and Smits, A.J., "Compilation of Turbulence Data for a 16° Compression Corner at Mach 2.9," Dept. of Mechanical and Aerospace Engineering, Princeton Univ., Princeton, NJ, MAE Rep. 1619, 1984.

[22] Muck, K.C., Spina, E.F., and Smits, A.J., "Compilation of Turbulence Data for an 8° Compression Corner at Mach 2.9," Dept. of Mechanical and Aerospace Engineering, Princeton Univ., Princeton, NJ, Rep. MAE-1642, 1984.

[23] Dolling, D., private communication, 1983.

[24] von Lavante, E. and Thompkins, W.T., "An Implicit Bi-diagonal Numerical Method for solving the Navier-Stokes Equations," AIAA Paper 82-0063, 1982.

[25] Pulliam, T. and Steger, J., "Implicit Finite-Difference Simulations of Three-Dimensional Compressible Flows," *AIAA Journal*, Vol. 18, Feb. 1980, pp. 159–167.

[26] Baldwin, B. and Lomax H., "Thin Layer Approximation and Algebraic Model for Separated Turbulent Flows," AIAA Paper 78-257, 1978.

[27] York, B. and Knight D., "Calculation of Two-Dimensional Turbulent Boundary Layers Using the Baldwin-Lomax Model," *AIAA Journal*, Vol. 23, Dec. 1985, pp. 1849–1850.

[28] Visbal, M. and Knight, D., "Generation of Orthogonal and Nearly Orthogonal Coordinates with Grid Control Near Boundaries," *AIAA Journal*, Vol. 20, March 1982, pp. 305–306.

[29] Thomas, P.D., "Boundary Conditions and Conservative Smoothing for Implicit Numerical Solutions to the Compressible Navier-Stokes Equations," Lockheed Missiles and Space Co., Palo Alto, CA, LMSC-D630729, 1978.

[30] Ong, C.C., "Calculation of Shock Wave-Turbulent Boundary Layer Interaction Over a Two-Dimensional Compression Corner," Ph.D. Thesis, Dept. of Mechanical and Aerospace Engineering, Rutgers Univ., New Brunswick, NJ, 1986.

[31] Shang, J.S., "Numerical Simulation of Wing-Fuselage Interference," AIAA Paper 81-0048, 1981.

[32] Tennekes, H. and Lumley, J., *A First Course in Turbulence*, MIT Press, Cambridge, MA, 1972.

[33] Dolling, D. and Murphy, M., "Wall Pressure Fluctuations in a Supersonic Separated Compression Ramp Flowfield," AIAA Paper 82-0986, 1982.

[34] Dolling, D. and Or, C.T., "Unsteadiness of the Shock Wave Structure in Attached and Separated Compression Ramp Flow Fields," AIAA Paper 83-1715, 1983.